*Original Research*

SCIENCE PROGRESS

Science Progress
2023, Vol. 106(3) 1–19

DOI: 10.1177/00368504231184320
journals.sagepub.com/home/sci

# Potential effects of brain lipid binding protein in the pathogenesis of amyotrophic lateral sclerosis

**Qi Zhou[1,*], Qing Kang[2,*], Wenzhi Chen[2,*] and Renshi Xu[2,*]**

[1]Department of Neurology, The First People's Hospital of Fuzhou City, Fuzhou, China
[2]Department of Neurology, Jiangxi Provincial People's Hospital, The Clinical College of Nanchang Medical College, The First Affiliated Hospital of Nanchang Medical College, Nanchang, China

## Abstract

Current studies suggest that the abnormal alteration of brain lipid binding protein (BLBP) might participate in the pathogenesis of amyotrophic lateral sclerosis (ALS). However, the detailed understanding of ALS pathogenesis been yet to be elucidated. Therefore, this research intended to explore the potential effects of BLBP in ALS. The observation and analysis of BLBP-altered features in various anatomical areas and different spinal segments was conducted at the pre-onset, onset, and progression stages of Tg(SOD1*G93A)1Gur (TG) mice and the same periods of age-matched SOD1 wild-type (WT) mice by fluorescence immunohistochemistry and western blotting. BLBP-positive cells were comprehensively distributed in various spinal anatomical areas, especially in both the anterior and posterior horn, around the central canal and in anterior, lateral, and posterior funiculi. Overall, BLBP expression tended to increase from the pre-onset to the onset to the progression stages of the same periods of age-matched WT mice. Furthermore, in TG mice, BLBP expression in the entire spinal cord significantly increased from onset to the progression stage. BLBP was expressed in neurons, astrocytes, and radial glial cells, and at the early and late stages of neural precursor cells (NPCs) and was predominantly distributed outside the cell nucleus. The increase of BLBP-positive cells was closely related to neural cell reduction in TG mice. The distribution and increased expression of BLBP among the cervical, thoracic, and lumbar segments of the spinal cord might participate in the development of ALS and exert potential effects in the pathogenesis of ALS by regulating NPCs.

*All the authors contributed equally to this work.

**Corresponding author:**
Renshi Xu, Department of Neurology, Jiangxi Provincial People's Hospital, The Clinical College of Nanchang Medical College, The First Affiliated Hospital of Nanchang Medical College, Nanchang 330006, China.
Email: 13767015770@163.com, xurenshi@ncu.edu.cn

**Keywords**
Amyotrophic lateral sclerosis, brain lipid binding protein, spinal cord, Tg(SOD1*G93A)1Gur mice, pathogenesis

## Introduction

Amyotrophic lateral sclerosis (ALS) is the most common motor-neuron disease among adult populations, and 95% of these ALS cases are idiopathic ALS. The characteristic pathological hallmark of ALS is the degeneration of both superior and inferior motor neurons in the cerebral cortex, brain stem, and spinal cord, which results in the progressive weakness and atrophy of muscle, and subsequently the progressive muscle paralysis of the whole body.[1] Most patients with ALS die approximately 4 years after the appearance of the first-onset symptom owing to the lack of effective treatments for this disease.[2]

Although the etiology of idiopathic ALS is partially unknown, the multiple gene mutations of Cu/Zn superoxide dismutase-1 (SOD1) were found to be related to approximately 20% of familial-type ALS cases.[3,4] Various mouse ALS-like transgene models were founded based on the mutations of SOD1 and have been extensively used to research the pathogenesis and possible treatments of ALS. Among them, the Tg(SOD1*G93A) 1Gur (TG) mouse model is an important model for studying the pathogenesis of ALS because its symptoms correspond to human ALS phenotypes.[5] It is not yet known why the ALS-like mouse models exhibit similar clinical manifestations and pathological changes of ALS in humans, including amyotrophy and the degenerative alteration of motor neurons. Moreover, an accurate link between the occurrence of symptoms and SOD1 mutation has not been identified to date.[5–8]

Brain lipid binding protein (BLBP) is comprehensively expressed among the radial glial cells (RGCs) of the central nervous system, glioblastomas, and U251 cells. The expression of BLBP exhibits a spatial and temporal relationship to neuronal differentiation among various regions of the mouse central nervous system, including postnatal cerebellum, embryo spinal cord, and cerebrum cortices. BLBP is transiently expressed among the RGCs of both the embryo ventricle area and postnatal cerebellum. Subcellular localization has shown that BLBP is present in the cell nucleus and cytoplasm. BLBP played a role in glial and neuronal differentiation.[9] BLBP, also known as fatty acid-binding protein 7, is a member of the family of fatty acid-binding proteins, which are involved in the cellular internal transportation of fatty acids.[10–12] As a transporter of fatty acids, the major functions of BLBP are the facilitation of cellular internal transportation of polyunsaturated fatty acids,[13] especially docosahexaenoic acids. In addition, BLBP binds arachidonic acid to express among various grades of human glioma and is closely related to promoting proliferation and modulating the cell cycle in glioma cells.[14,15]

Proteins known to be associated with ALS include SOD1, TDP-43, FUS, and c9orf72.[16–19] However, it is anticipated that several other proteins involved in ALS are still awaiting discovery. Our previous study revealed that BLBP was involved in spinal damage in TG mice,[20] but the relevance between neuron death and BLBP is not known. Therefore, in the current study, we further investigated the relevance of BLBP

for the pathological mechanism of motor neuronal degeneration by investigating the expression level and localization of BLBP in different spinal anatomical areas at various stages of ALS-like disease in TG mice.

## Materials and methods

### Animal model

C57BL/6J Tg(SOD1*G93A)1Gur (TG) mice derived from the Model Animal Research Center of Nanjing University were bred by mating male TG mice with wild-type (WT) C57BL/6J female mice.[5] TG mice were confirmed by polymerase chain reaction (PCR) using genomic DNA isolated from mouse tails. Primers used in PCR were: interleukin (IL)-2 forward primer 5′-CTAGGCCACAGAATTGAAAGATCT-3′, IL-2 reverse primer 5′-GTAGGTGGAAATTCTAGCATCATCC-3′, hmSOD1 forward primer 5′-CATCAGCCCTAATCCATCTGA-3′, and hmSOD1 reverse primer 5′-CGCGACTAACAATCAAAGTGA-3′. The PCR comprised 35 cycles of 3s degeneration at 94°C, 1 min annealing at 60°C, and 1 min extension at 72°C.

The ALS-like model was divided into three disease stages: pre-onset (60–70 days), onset (90–100 days), and progression (120–130 days).[5,21] Gastrocnemius muscle biopsy was used to detect abnormal alteration scale to further define disease stages.[22] All animal experiments were reviewed and approved by the Institutional Animal Care and Use Committee (IACUC ID is 2019063002) of Jiangxi Provincial People's Hospital.

### Fluorescent immunohistochemical stain of spinal cord

WT and TG mice were anesthetized and perfused using 20 mL of 0.9% saline and 40 mL of 4% paraformaldehyde (PFA) in 1× phosphate-buffered saline (PBS) (pH 7.5) at room temperature (RT). Spinal cords were excised, placed in 4% PFA buffer overnight, then incubated in 20% sucrose in 1× PBS (pH 7.5) and embedded using optimal cutting temperature compound. Samples were cut into 12μm successive coronal sections and collected on Superfrost Plus slides. For fluorescent immunohistochemical staining, sections were permeabilized with 0.2% Triton X-100, blocked with 10% goat serum in 1× PBS after rehydrating in 1× PBS (pH 7.4), and incubated with primary antibodies to Vimentin (1:200), Fox 3 (1:200), glial fibrillary acidic protein astrocytopathy (GFAP) (1:1000), Nestin (1:200), and BLBP (1:200) (Abcam (Hong Kong) Ltd) at 4°C overnight. Subsequently, samples were washed 6 times with 0.2% Triton X-100 in 1× PBS (5 min for each wash), incubated with secondary antibodies donkey anti-goat (1:250) and donkey anti-rabbit (1:200) conjugated to fluorescein (green) or/and rhodamine (red) for 2 h at RT, and then stained with 4′,6-diamidino-2-phenylindole (DAPI; blue). All stained sections were extensively washed in 0.2% Triton X-100 in 1× PBS, mounted in anti-fade medium, and observed and photographed using a Nikon E800 fluorescent microscope equipped with a spot digital camera (Diagnostic Instruments, Sterling Heights, MI, USA) and Photoshop software (Adobe Systems, San Jose, CA, USA). An autofluorescence quenching agent (AutoFluo Quencher C1212; Beijing APPLYGEN Technologies Inc., Beijing, China) was applied to all samples.

### Relationship of BLBP to particular cell types

A multilabeling fluorescent immunohistochemical method was applied to achieve double or triple staining in the same sample. Primary antibodies to different biomarkers including BLBP, Fox3, GFAP, Nestin, and Vimentin, and the corresponding secondary antibodies conjugated to different color fluorescence. DAPI was used for immunohistochemical staining. BLBP distribution in different neural cells was examined by observing the overlapping of different color fluorescence. Second antibodies were regularly applied for staining no primary antibody samples to use for evaluating the negative controls of primary antibody validity.

### Bromodeoxyuridine administration and staining of spinal cord

To detect neurogenesis in spinal cord, bromodeoxyuridine (BrdU; 50 mg/kg) was intraperitoneally injected into WT and TG mice twice, with a 12h interval between the doses. The concentration of BrdU solution was 10 mg/mL. After injection with BrdU, animals were continued to breed for 7 days, then were killed and the samples of spinal cord were prepared, fixed, embedded, and sliced under dark conditions. The details of the fluorescent immunohistochemical staining protocol were as described above.

### Analysis of fluorescent immunohistochemical BLBP-positive cells

Following fluorescent immunohistochemical staining, the number of BLBP-positive cells in the sections of spinal cord was counted under 200× magnification based on the mice anatomic atlas by the version 6.0 Image-Pro Plus software (Media Cybernetics, Silver Springs, MD, USA). The mean number of BLP-positive cells per section was calculated. There were three mice per group and three sections per mouse.

### Analysis of neural cell reduction

Analysis of neural cell reduction was conducted by counting the number of neural cells under 200× magnification among three stained sections based on the mice anatomic atlas by the version 6.0 Image-Pro Plus software (Media Cybernetics, Silver Springs, MD, USA), calculated the mean number of neural cells per section. There were three mice per group and three sections per mouse.

### Western blot

WT and TG mice were anesthetized and perfused by 20 mL of 0.9% saline. Spinal cords were excised and homogenized in ice-cold 1×radioimmunoprecipitation assay lysis buffer (150 mM NaCl, 1% Nonidet P-40, 12 mM sodium deoxycolate, 0.1% sodium dodecyl sulfate (SDS), and 50 mM Tris-HCl; pH 7.2) supplemented with protease inhibitor. The resulting lysate was centrifuged at 12,000 ×$g$ at 4°C for 10 min. The supernatant was collected for the western blotting (WB) analysis of BLBP. The protein concentration of samples was measured by bicinchoninic acid Protein Assay Kit (Solarbio, Beijing, China)

and 20 μg protein was subsequently loaded into each well of 10% SDS-polyacrylamide gels, electrophoresed, and then transferred onto nitrocellulose membranes (Millipore, Bedford, MA, USA). Membranes were blocked with 5% bovine serum albumin Tris-buffered saline (TBST) (10 mM Tris-HCl, pH 7.5, 150 mM NaCl, 0.1% Tween 20) for 1 h at RT, then incubated with antibodies BLBP (1:1000; Abcam, Hong Kong Ltd) and beta-actin (1:5000; Proteintech Group, Wuhan, China) at 4°C overnight. Membranes were washed three times for 5 min each time in TBST at RT, and then incubated with horseradish peroxidase-labeled goat anti-rabbit IgG (Beyotime, Shanghai, China) for 1 h at RT. Finally, membranes were washed three times for 5 min each time in TBST and were visualized by BeyoECL Plus Kit (Beyotime, Shanghai, China). The optical density of WB bands was measured by Quantity One 1-D Analysis software (Bio-Rad Laboratories, Inc.). Three mice per group were used and experiments were repeated three times.

### *Statistical analysis*

All data were expressed as mean ± standard error of the mean. Statistical analyses were conducted using SPSS (Version 17.0) statistical software (SPSS, Chicago, IL, USA). Specific comparisons between controls and experimental groups were analyzed by the analysis of variance (ANOVA), including the multivariate ANOVA. Two-way ANOVA and eventual Post Hoc test were applied for paired comparisons including the group of different anatomical regions and the group of different disease stages. Each data set of groups passed a test for Gaussian distribution. $P<0.05$ was considered statistically significant.

## Results

### *BLBP-positive cell alterations in different spinal segments and anatomical regions of spinal cord at different stages of TG mice and the same periods of age-matched WT mice*

In the anterior horn (AH) of WT mice, there were significantly more BLBP-positive cells in both thoracic and lumbar segments compared with those in the cervical segment at the pre-onset same period of age-matched WT mice. At the same periods of onset stage of age-matched WT mice, there were significantly more BLBP-positive cells in the lumbar segment compared with the cervical and thoracic segments, while at the progression stage same period of age-matched WT mice, there were significantly more BLBP-positive cells in the cervical segment compared with those in the thoracic and lumbar segments. In the AH of TG mice, there were significantly more BLBP-positive cells in both thoracic and lumbar segments compared with those in the cervical segment at both pre-onset and onset stages. At the progression stage, there were significantly more BLBP-positive cells in the cervical and lumbar segments compared to those in the thoracic segment. The comparison of the AH of WT and TG mice revealed that there were significantly more BLBP-positive cells in the cervical, thoracic, and lumbar segments of TG mice compared with those in WT mouse at the pre-onset stage. In addition, the cervical and thoracic segments in TG mice contained significantly more

BLBP-positive cells compared with WT mice at the onset stage, and there were significantly more BLBP-positive cells in the lumbar segment of TG mice at the progression stage compared with that of WT mice (Figure 1A and B).

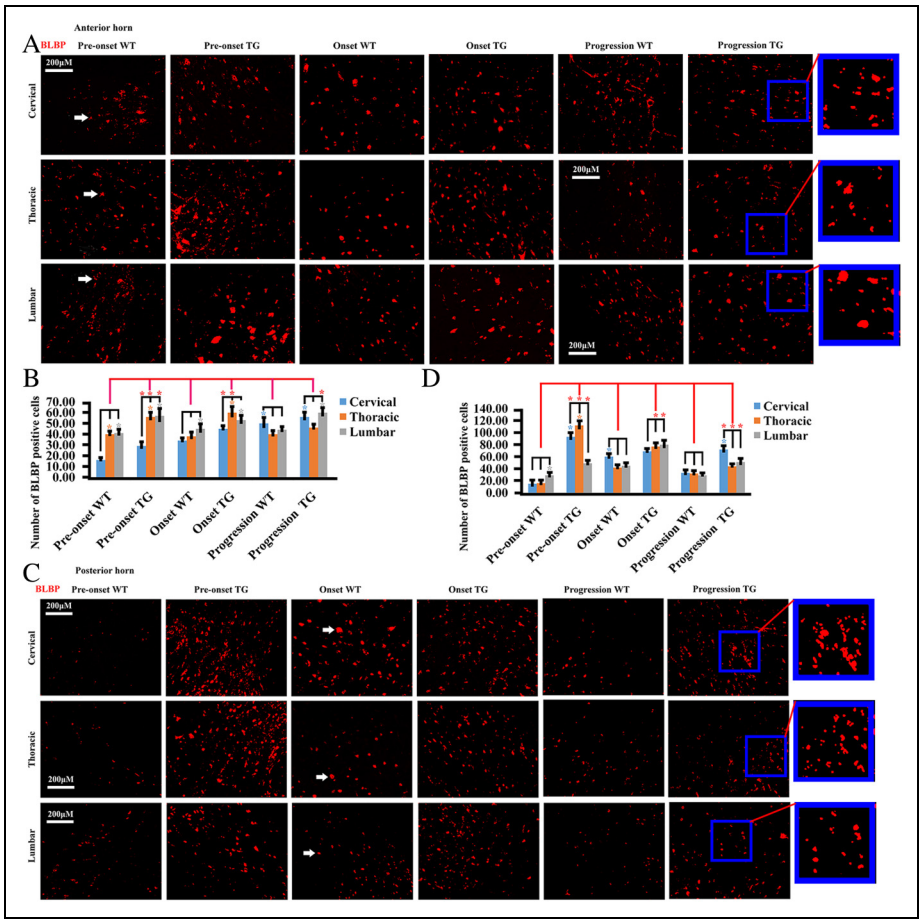


**Figure 1.** The analysis of the distribution of BLBP-positive cells in the AH and PH of cervical, thoracic, and lumbar segments of spinal cord at different stages of TG mice and the same periods of age-matched WT mice. (A) The representative fluorescent immunohistochemical images of BLBP-positive cells in AH. Bar (amplified 20 times, 20×), 200 μM. White arrow indicates BLBP-positive cells. (B) The quantitative analysis of BLBP-positive cells in AH. (C) The representative fluorescent immunohistochemical images of BLBP-positive cells in PH. White arrow indicates BLBP-positive cells. (D) The quantitative analysis of BLBP-positive cells in PH. Asterisk indicates statistically significant differences at $P<0.05$. Different color asterisks represent the column graph color of correspondence group, indicate that this group is significantly different compared with corresponding group. Red asterisk represents a comparative statistical significance between WT and TG groups. AH: anterior horn; BLBP: brain lipid binding protein; PH: posterior horn; TG: Tg(SOD1*G93A)1Gur; WT: wild-type.

Among the posterior horn (PH) of WT mice, there were significantly more BLBP-positive cells in the lumbar segment compared with the cervical and thoracic segments at the pre-onset stage same period of age-matched WT mice, and the number of BLBP-positive cells in the cervical segment was significantly greater compared with that in the thoracic and lumbar segments at the onset stage same period of age-matched WT mice. In the PH of TG mice, there were significantly more BLBP-positive cells in the cervical and thoracic segments compared with those in the lumbar segment at the pre-onset stage. There were also significantly more BLBP-positive cells in the cervical segment compared with those in the thoracic and lumbar segments at the progression stage. The comparison of the PH of WT and TG mice revealed that there were significantly more BLBP-positive cells in the cervical, thoracic, and lumbar segments of TG mice at both pre-onset and progression stages and at the onset stage, both thoracic and lumbar segments of TG mice contained significantly more BLBP-positive cells compared with those in WT mice (Figure 1C and D).

Among the central canal (CC) of WT mice, there were significantly more BLBP-positive cells in the cervical segment compared with those in the thoracic and lumbar segments at the onset stage same period of age-matched WT mice, and BLBP-positive cells in the lumbar segment were significantly more than that in the cervical segment more than that in the thoracic segment at the progression stage same period of age-matched WT mice. In the CC of TG mice, there were significantly more BLBP-positive cells in the cervical segment compared with those in the thoracic segment at the pre-onset stage, and significantly more in both the cervical and lumbar segments compared with those in the thoracic segment at the progression stage. The comparison of the CC of WT and TG mice revealed that there were significantly more BLBP-positive cells in the cervical, thoracic, and lumbar segments of TG mice at the pre-onset stage, significantly fewer BLBP-positive cells in the thoracic and lumbar segments of TG mice compared with those of WT mice at onset stage, and significantly more BLBP-positive cells in the cervical and lumbar segments of TG mice at progression stage (Figure 2A and B).

Among the anterior funiculus (AF) of WT mice, there were significantly more BLBP-positive cells in the thoracic and lumbar segments compared with those in the cervical segment at the pre-onset stage same period of age-matched WT mice, significantly more BLBP-positive cells in the thoracic segment compared with those in both cervical and lumbar segments at the onset stage same period of age-matched WT mice, and significantly more BLBP-positive cells in the lumbar segment compared with those in the cervical and thoracic segments at the progression stage same period of age-matched WT mice. In the AF of TG mice, there were significantly more BLBP-positive cells in the thoracic segment compared with those in the cervical and lumbar segments at the pre-onset stage, significantly more BLBP-positive cells in the thoracic and lumbar segments compared with those in the cervical segment at onset stage, and significantly more BLBP-positive cells in both cervical and lumbar segments compared with those in the thoracic segment at progression stage. The comparison of the AF of WT and TG mice revealed that there were significantly more BLBP-positive cells in the cervical and thoracic segments of TG mice at the pre-onset stage, significantly more BLBP-positive cells in the thoracic and lumbar segments of TG mice at the onset stage, and significantly more BLBP-positive cells in the cervical, thoracic, and lumbar segments of TG mice at progression stage (Figure 2C and D).

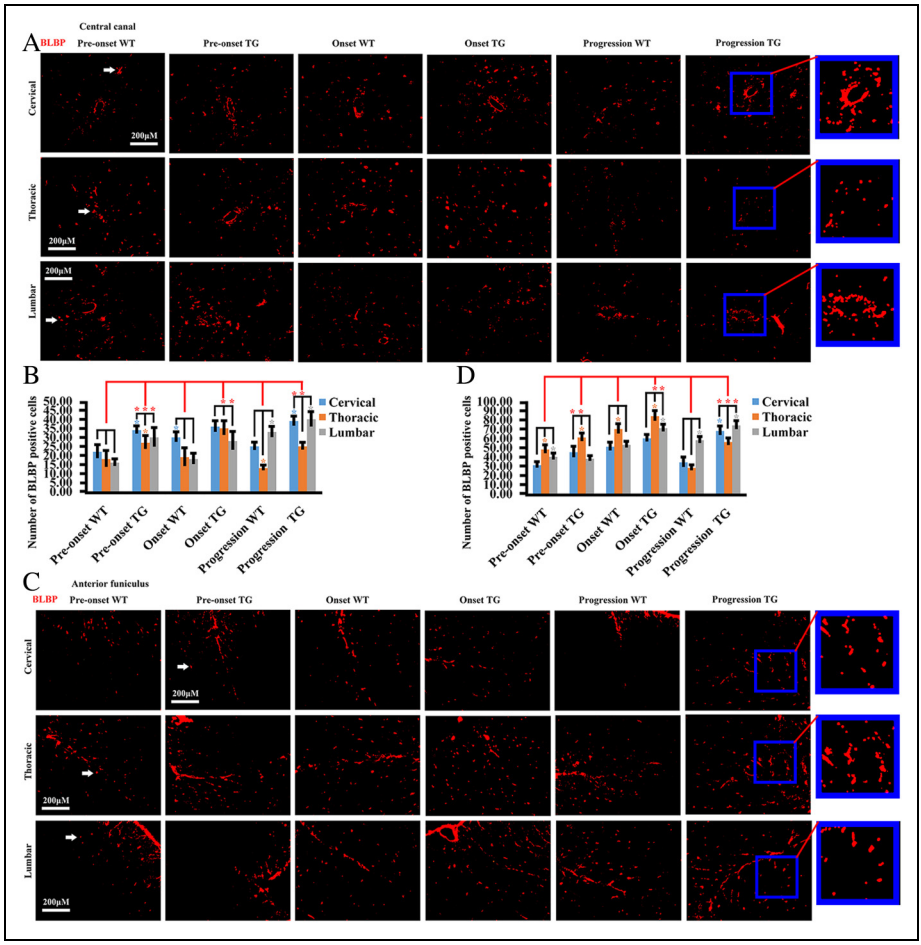


**Figure 2.** The quantitative analysis of the distribution of BLBP-positive cells in CC and AF of cervical, thoracic, and lumbar segments of spinal cord at different stages of TG mice and the same periods of age-matched WT mice. (A) The representative fluorescent immunohistochemical images of BLBP-positive cells in CC. (B) The quantitative analysis of BLBP-positive cells in CC. (C) The representative fluorescent immunohistochemical images of BLBP-positive cells in AF. (D) The quantitative analysis of BLBP-positive cells in AF. White arrow points to BLBP-positive cells. Asterisk indicates statistically significant differences at $P<0.05$. Different colored asterisks represent the column graph color of correspondence group, indicate that this group is significantly different compared with corresponding group. Red asterisk represents a comparative statistical significance between WT and TG groups. AF: anterior funiculus; BLBP: brain lipid binding protein; CC: central canal; TG: Tg(SOD1*G93A)1Gur; WT: wild-type.

Among the lateral funiculus (LF) of WT mice, there were more BLBP-positive cells in the cervical segment compared with the thoracic and lumbar segments at the pre-onset stage, the number of BLBP-positive cells in the cervical segment was significantly

more than that in the thoracic segment and more than that in the lumbar segment at the pre-onset stage same period of age-matched WT mice. In addition, there were significantly more BLBP-positive cells in the thoracic segment compared with those in the cervical and lumbar segments at both onset and progression stages same period of age-matched WT mice. In the LF of TG mice, there were significantly more BLBP-positive cells in the cervical and thoracic segments compared with those in the lumbar segment at the pre-onset stage, and significantly more BLBP-positive cells in both thoracic and lumbar segments compared with those in the cervical segments at progression stage. The comparison of the LF of WT mice with that of TG mice revealed that there were significantly fewer BLBP-positive cells in the cervical and lumbar segments of TG mice at the pre-onset stage, and significantly fewer BLBP-positive cells in the cervical and thoracic segments of TG mice at both onset and progression stages (Figure 3A and B).

Among the posterior funiculus (PF) of WT mice, there were more BLBP-positive cells in the lumbar segment compared with the thoracic and cervical segments at the pre-onset stage, the number of BLBP-positive cells in the lumbar segment was significantly more than that in the thoracic segment more than that in the cervical segment at the pre-onset stage same period of age-matched WT mice. Furthermore, there were significantly more BLBP-positive cells in the thoracic and lumbar segments compared with those in the cervical segment at the onset stage same period of age-matched WT mice, and significantly more BLBP-positive cells in the lumbar segment compared with those in the cervical and thoracic segments at the progression stage same period of age-matched WT mice. In the PF of TG mice, there were significantly more BLBP-positive cells in the thoracic and lumbar segments compared with those in the cervical segment at the pre-onset stage. In addition, there were significantly more BLBP-positive cells in the thoracic segment compared with those in the cervical and lumbar segments at the onset stage, and significantly more BLBP-positive cells in both the thoracic and lumbar segments compared with those in the cervical segment at the progression stage. The comparison of the PF of WT mice with that of TG mice revealed that there were significantly fewer BLBP-positive cells in the lumbar segment of TG mice at the pre-onset stage, and significantly fewer BLBP-positive cells in all three segments of TG mice at both onset and progression stages (Figure 3C and D).

## *Alteration of BrdU-positive cells in different spinal segments at the different stages of TG mice and the same periods of age-matched WT mice*

In WT mice, there were significantly more BrdU-positive cells (BPCs) in the lumbar segment compared with those in the cervical segment at the onset stage same period of age-matched WT mice, and significantly more BPCs in both thoracic and lumbar segments compared with those in the cervical segment at the progression stage same period of age-matched WT mice. With the increase in age of the mice, there was a relative increase in BPCs in the thoracic and lumbar segments accompanied by a decrease in BPCs in the cervical segment. In TG mice, there were significantly more BPCs in the lumbar segment compared with those in the cervical and thoracic segments at both pre-onset and progression stages, and significantly more BPCs in the cervical and lumbar

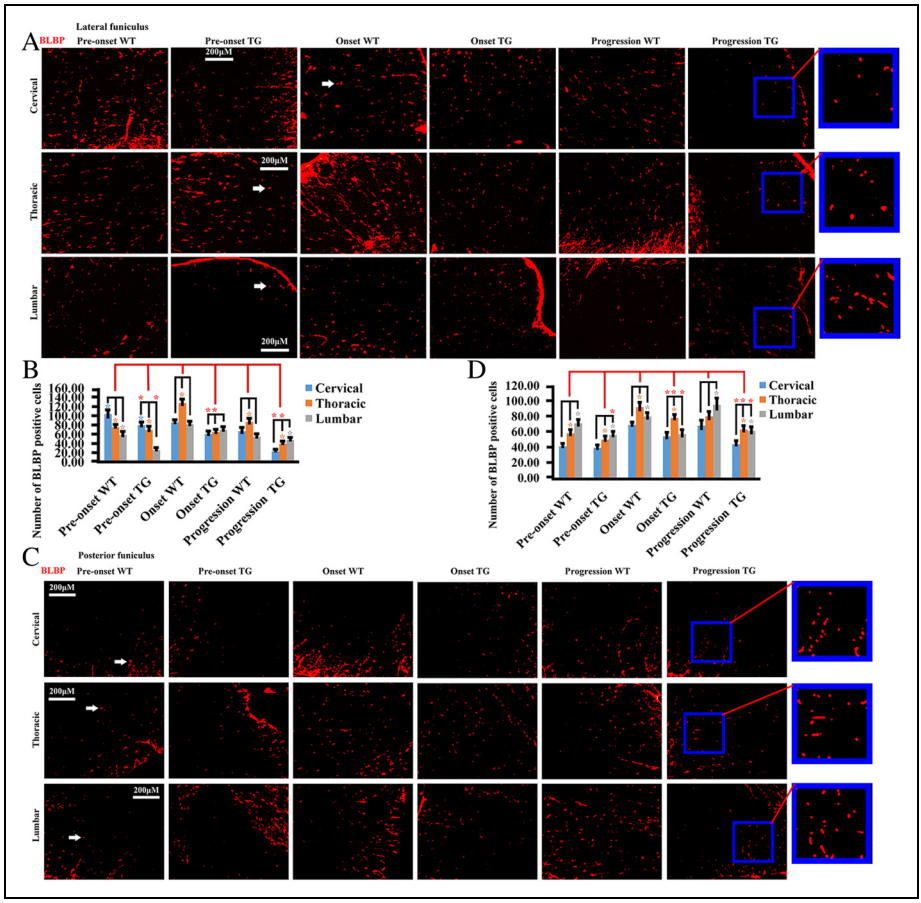


**Figure 3.** The quantitative analysis of the distribution of BLBP-positive cells in LF and PF of cervical, thoracic, and lumbar segments of spinal cord at different stages of TG mice and the same periods of age-matched WT mice. (A) The representative fluorescent immunohistochemical images of BLBP-positive cells in LF. (B) The quantitative analysis of BLBP-positive cells in LF. (C) The representative fluorescent immunohistochemical images of BLBP-positive cells in PF. (D) The quantitative analysis of BLBP-positive cells in PF. White arrow indicates BLBP-positive cells. Asterisk indicates statistically significant differences at $P<0.05$. Different colored asterisks represent the column graph color of correspondence group, indicate that this group is significantly different compared with corresponding group. Red asterisk represents a comparative statistical significance between WT and TG groups. BLBP: brain lipid binding protein; LF: lateral funiculi; PF: posterior funiculi; TG: Tg(SOD1*G93A)1Gur; WT: wild-type.

segments compared with those in the thoracic segment at onset stage. BPCs in the lumbar segment significantly increased with the development of ALS from pre-onset to onset to progression stages, while those in the cervical segment significantly increased at the onset stage. The comparison of WT mice with TG mice revealed that there were significantly more BPCs in all three spinal segments of TG mice at all three disease stages, indicating

that BPCs exhibited an increasing trend through the ALS developmental course in the cervical, thoracic, and lumbar segments (Figure 4).

## *Overlap staining of BLBP, DAPI, Fox3, GFAP, Nestin, and Vimentin*

BLBP showed partial overlap of staining with Fox3 (Figure 5A), GFAP (Figure 5B), Nestin (Figure 5D), and Vimentin (Figure 5E) in CC and surrounding CC and LF. BLBP was predominantly distributed in neurons, astrocytes or RGCs, and neural precursor cells (NPCs) in CC and surrounding CC and LF. BLBP did not exhibit double staining with DAPI, indicating that BLBP was predominantly distributed on the outside of the cell nucleus, with a small amount of BLBP staining detected in the cell nucleus (Figure 5C and F).

## *Alteration of BLBP expression in the entire spinal cord at the different stages of TG mice and the same periods of age-matched WT mice*

In WT mice, BLBP expression in the entire spinal cord at the progression stage same period of age-matched WT mice was significantly more than that at onset stage same

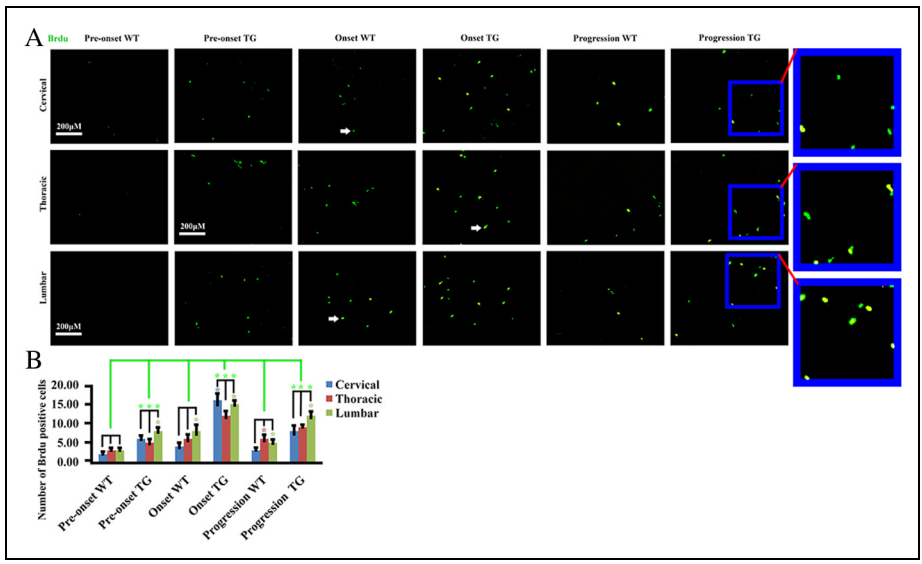


**Figure 4.** The quantitative analysis of the distribution of BPCs in the cervical, thoracic, and lumbar segments of spinal cord at the different stages of TG mice and the same periods of age-matched WT mice. (A) The representative fluorescent immunohistochemical images of BPCs. Bar (20×), 200 μM. White arrow indicates BPCs. (B) The quantitative analysis of BPCs. All asterisks on graphs indicate a comparative statistical significance at $P<0.05$, different colored asterisks represent the column graph color of correspondence group, indicate that this group is significantly different compared with corresponding group. Green asterisk represents a comparative statistical significance between WT and TG groups. BPC: BrdU-positive cells; TG: Tg(SOD1*G93A)1Gur; WT: wild-type.

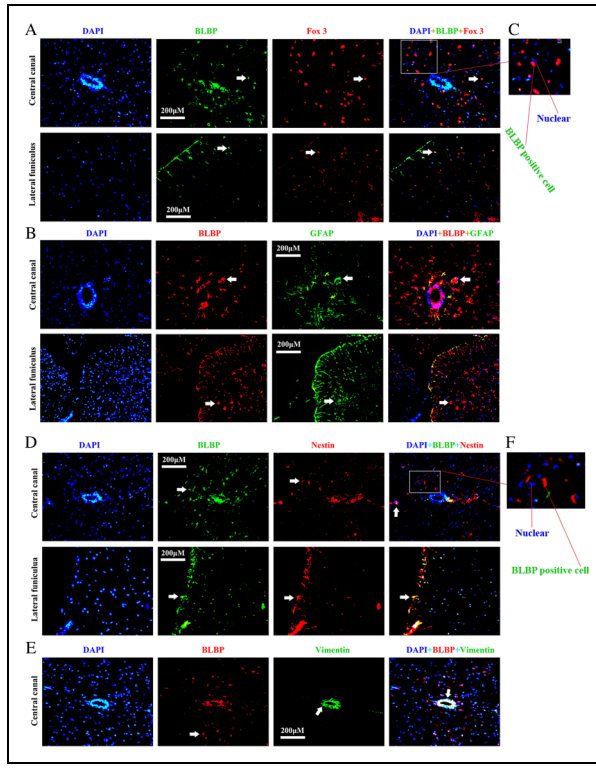


**Figure 5.** The overlapped staining of BLBP, DAPI, Fox3 and GFAP, and BLBP, DAPI, Nestin and Vimentin in the spinal cord of WT and TG mice. (A) The representative image of BLBP and Fox3 staining in central canal (CC) and lateral funiculus (LF). BLBP-positive cells show partial double staining with Fox3, indicating that BLBP is partially expressed in neurons. White arrow points to BLBP-positive, DAPI-positive, and Fox3-positive cells and triple-positive cells for BLBP, DAPI, and Fox3. (B) The representative image of BLBP and GFAP staining in CC and LF. BLBP-positive cells show partial double staining with GFAP, indicating that BLBP is partially expressed in astrocytes or RGCs. White arrow indicates BLBP-positive, DAPI-positive, and Fox3-positive cells and triple-positive cells for BLBP, DAPI, and GFAP. (C) The representative image of BLBP and DAPI staining in CC. Most BLBP-positive cells did not exhibit overlapping staining with DAPI, indicating that BLBP is predominantly distributed outside of neural cell nucleus. (D) The representative image of BLBP and Nestin staining in CC and LF. BLBP-positive cells showed partial double staining with Nestin, indicating that BLBP is partially expressed at the early stage of NPCs. White arrow points to BLBP-positive, DAPI-positive, and Nestin-positive cells and the cells triple stained with BLBP, DAPI, and Nestin. (E) The representative image of BLBP and Vimentin staining in CC. BLBP-positive cells showed partial double staining with Vimentin, indicating that BLBP is partially expressed at the later stage of NPCs. White arrow points to BLBP-positive, DAPI-positive, and Vimentin-positive cells and the cells triple stained with BLBP, DAPI, and Vimentin. (F) The representative image of BLBP and DAPI in CC. Almost all BLBP-positive cells did not exhibit double staining with DAPI, indicating that BLBP is predominantly distributed outside of neural cell nucleus. BLBP: brain lipid binding protein; CC: central canal; DAPI: 4′,6-diamidino-2-phenylindole; LF: lateral funiculi; NPC: neural precursor cell; RGC: radial glial cell; TG: Tg(SOD1*G93A)1Gur; WT: wild-type.

period of age-matched WT mice significantly more than that at the pre-onset stage same period of age-matched WT mice (BLBP expression in the entire spinal cord at the progression stage of age-matched WT mice > that at onset stage same period > that at pre-onset stage same period), which showed a gradually increasing tendency with increasing age (Figure 6A and B). BLBP expression in the entire spinal cord also significantly increased from pre-onset to onset to progression stages in TG mice. In addition, BLBP expression in TG mice at both onset and progression stages was significantly greater compared with that at the same period in WT mice (Figure 6C and D).

### *Relationship of BLBP-positive cells and number of neural cells in different spinal segments at the different stages of TG mice and the same periods of age-matched WT mice*

A reduction in the number of neural cells was closely associated with the increase in BLBP-positive cells in neurons and astrocytes or RGCs of the cervical, thoracic and lumbar segments in TG mice, which implied that the alteration of BLBP was closely related to neural cell reduction (Figure 6E). This finding emphasized that an increase in BLBP is potentially involved in the mechanism of neural cell reduction in the pathogenesis of ALS.

## Discussion

Several conclusions were derived based on the experimental results of this study. Firstly, at normal physiologic conditions, BLBP was extensively distributed in AH, PH, around CC, AF, LF, and PF. BLBP was expressed in neurons and astrocytes or RGCs and in early and late-stage NPCs and was predominantly distributed outside the nucleus of neural cells, with a small amount detected in the cell nucleus. In addition, BLBP expression significantly increased with increasing age. Secondly, in an ALS-like pathological condition, BLBP expression in the entire spinal cord significantly increased from pre-onset to onset to progression stages of the disease. BLBP expression tended to be increased in AH and PH, CC and its surroundings, AF, LF and PF of cervical, thoracic and lumbar segments, and significant differences in BLBP expression were observed between cervical, thoracic, and lumbar segments. Finally, the distribution of BLBP-positive cells was closely associated with neural cell reduction over the developing course of ALS, and BLBP participated in the pathogenesis of neural cell reduction in ALS.

BLBP is a well-known biomarker of neural stem cells and RGCs in the central nervous system. In the embryo brain, BLBP is necessary for the maintenance and proliferation of NSC, NPCs, and RGCs.[23,24] Furthermore, BLBP expression was the downstream signal of both *PAX6* and *NOTCH* genes.[25,26] In the adult brain, BLBP is expressed in astrocyte and oligodendrocyte precursor cells and participates in the proliferation of astrocytes among normal and stab-injured cerebral cortices.[12] BLBP-expressing astrocytes regulate the morphology of dendrites and the functions of excitatory synapses in cortical neurons.[27] In the adult spinal cord, BLBP is expressed in the pial bound of

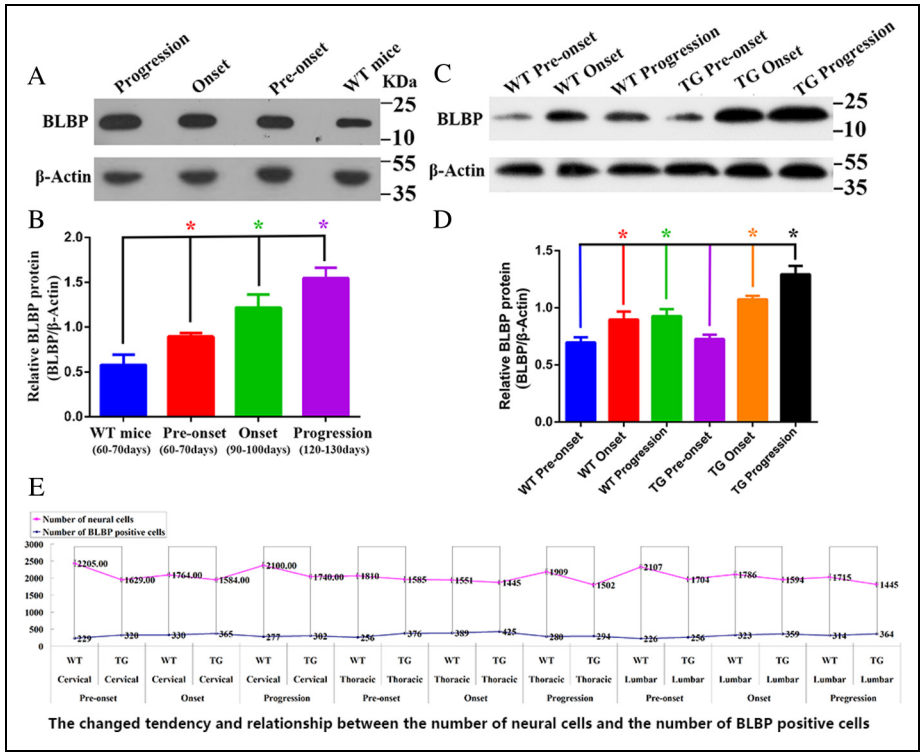


**Figure 6.** The comparison of BLBP expression in entire spinal cord at the different stages of TG mice and the same periods of age-matched WT mice. (A) The WB analysis of BLBP expression in entire spinal cord at the pre-onset, onset, and progression same periods of age-matched WT mice. (B) The quantitative analysis of BLBP WB showed that BLBP expression significantly increased with increasing age. (C) The WB analysis of BLBP expression in entire spinal cord at the pre-onset, onset, and progression stages of TG mice and the same periods of age-matched WT mice. (D) The quantitative analysis of BLBP WB showed that BLBP expression in entire spinal cord significantly increased from pre-onset stage to progression stage, and BLBP expression in entire spinal cord significantly increased at both onset and progression stages of TG mice compared with the same periods of age-matched WT mice. All asterisks on graphs indicate a comparative statistical significance at $P<0.05$, different color asterisks represent the column graph color of correspondence group, indicate that this group is significantly different compared with corresponding group. (E) Relationship between BLBP-positive cells and neural cell reduction in the cervical, thoracic and lumbar segments of spinal cord at the different stages of TG mice and the same periods of age-matched WT mice. The increase of BLBP-positive cells was accompanied by an increase of neural cell reduction in the cervical, thoracic and lumbar segments at the pre-onset, onset, and progression stages of TG mice compared with the same periods of age-matched WT mice. BLBP: brain lipid binding protein; TG: Tg(SOD1*G93A)1Gur; WB: western blotting; WT: wild-type.

GFAP-positive cells and plays important roles in numerous neurodegenerative diseases including ALS.[11] Immunohistochemical staining and analysis in the current study showed that BLBP expression overlapped with that of GFAP (RGCs and astrocytes

molecular marker), Nestin, and Vimentin (molecular marker of NPCs), demonstrating that BLBP was expressed in RGCs and NPCs. This indicated that BLBP participated in the differentiation of neurons and glial cells in the adult spinal cord.

In the early postnatal period, RGCs develop into GFAP+ astrocytes.[28] BLBP/GFAP-positive doubly labeled cells were previously reported to be predominantly detected in the outer layer of cortices extending to the pial surface as well as in cells distributed adjacent to ventricles.[28] In the present study, BLBP was expressed in the GFAP+ cells and RGCs of spinal CC, and BLBP expression in CC exhibited an increasing tendency, while RGCs in the spinal cord showed a decreasing tendency (Figure 5B). This

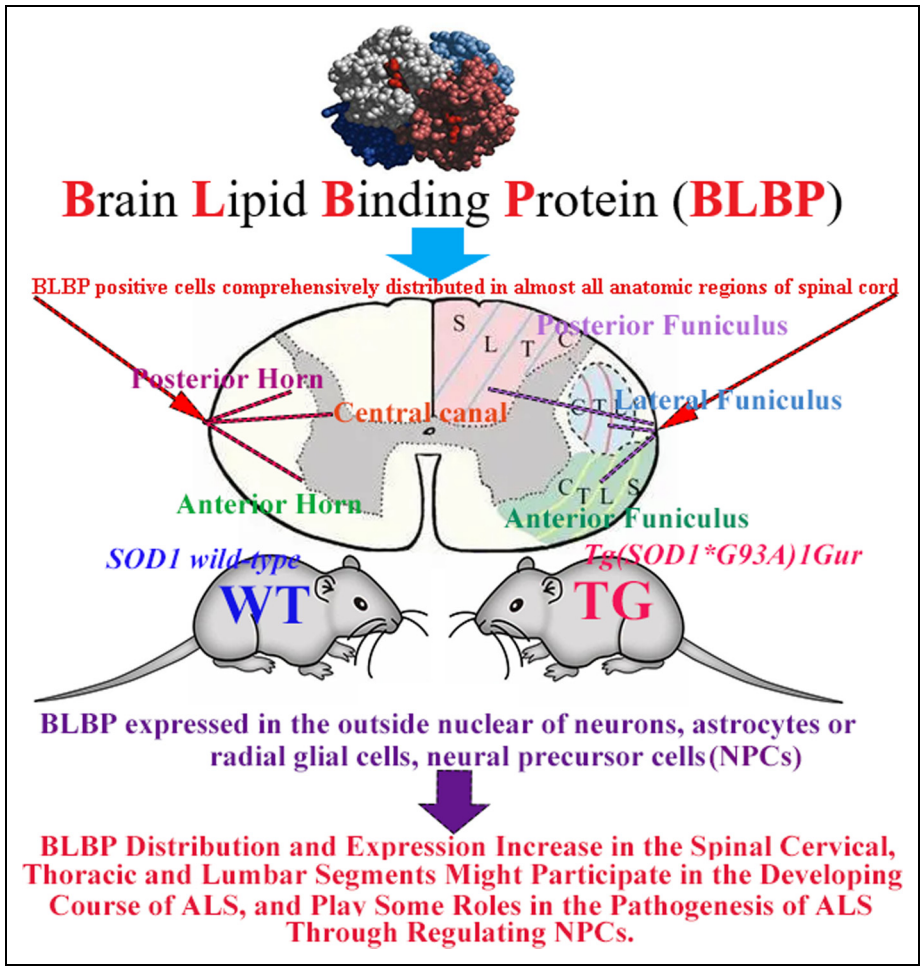


**Figure 7.** Schematics illustrating how both distribution and increased expression of BLBP among the cervical, thoracic, and lumbar segments of spinal cord participates in the developing course of ALS and exerts potential effects in the pathogenesis of ALS by regulating NPCs. ALS: amyotrophic lateral sclerosis; BLBP: brain lipid binding protein; NPC: neural precursor cell.

implies that RGCs in CC might transform into GFAP+ astrocytes to self-repair neural cell lesions through the action of BLBP.

BLBP binds long-chain fatty acids and other hydrophobic ligands, has essential roles in the uptake and transport of fatty acids, and participates in their metabolism. The ω-3 docosahexaenoic acid was reported as the preferred ligand of BLBP, but BLBP can also bind ω-6 arachidonic acid.[14] Highly unsaturated long-chain fatty acids alter the structure and functions of membranes, increasing their fluidity, elasticity and permeability, as well as potentially affecting signal transduction and gene expression.[29–32] The present study determined that BLBP participated in the pathogenesis of ALS. Based on previously reported research,[29–32] we conjectured that ALS pathogenesis might exhibit some association with the uptake and transport metabolism of long-chain fatty acids, altering the structure and functions of membranes, which increased their fluidity, elasticity and permeability, and potentially affecting signal transduction and gene expression via BLBP binding to its ligands such as polyunsaturated fatty acid, ω-3 docosahexaenoic acid and ω-6 arachidonic acid.

Furthermore, BLBP is also expressed in malignant glioma cell lines such as U251 cells, and exogenous BLBP enhances the motility and migration of U87 cells.[32] The expression of BLBP was previously reported to be controlled by peroxisome proliferator-activated receptors[33,34] and PAX6,[26] and nuclear factor I also controls the proliferation and cycle arresting of cells through modulation of p16, p21, and p27. Exogenous BLBP enhanced the migration abilities of U87 cells.[35] Migrating behaviors induced by BLBP expression are dependent on cyclooxygenase 2 expression.[36] The current study found that BLBP was expressed in neurons, astrocytes, RGCs, and NPCs, however, it has yet to be determined whether BLBP enhances the motility and migration of these cells through the above-described modulating and controlling mechanisms of malignant glioma cells. This will be explored in future research to potentially provide some novel clues regarding ALS pathogenesis.

## Conclusion

This study is a preliminary experimental investigation exploring the relationship between BLBP and ALS. BLBP distribution and expression features in the adult spinal cord of mice were obtained under both physiological and ALS pathological conditions, BLBP was found to participate in the pathogenesis of ALS, thus, BLBP is a potential treatment target for ALS (Figure 7).

### Authors contributions

QZ and QK contributed to conceptualization, visualization, and writing-original draft, review and editing. WC contributed to writing-review and editing. RX contributed to supervision, funding acquisition, and writing-review and editing. All authors contributed to the article and approved the submitted version.

### Declaration of conflicting interests

The author(s) declare that the research was conducted in the absence of any commercial or financial relationships that could be construed as a potential conflict of interest.

## Funding

The author(s) disclosed receipt of the following financial support for the research, authorship, and/or publication of this article: This work was supported by the National Natural Science Foundation of China (30560042, 81160161, 81360198, and 82160255), Education Department of Jiangxi Province (GJJ13198 and GJJ170021), Jiangxi Provincial Department of Science and Technology ([2014]-47, 20142BBG70062, 20171BAB215022, and 20192BAB205043), and Health and Family Planning Commission of Jiangxi Province (20181019).

## ORCID iD


Renshi Xu https://orcid.org/0000-0003-0313-3434

## References

1. Cozzolino M and Carrì MT. Mitochondrial dysfunction in ALS. *Prog Neurobiol* 2012; 97: 54–66.
2. Kiernan MC, Vucic S, Cheah BC, et al. Amyotrophic lateral sclerosis. *Lancet* 2011; 377: 942–955.
3. Kaur SJ, McKeown SR and Rashid S. Mutant SOD1 mediated pathogenesis of amyotrophic lateral sclerosis. *Gene* 2016; 577: 109–118.
4. Suzuki N, Nishiyama A, Warita H, et al. Genetics of amyotrophic lateral sclerosis: seeking therapeutic targets in the era of gene therapy. *J Hum Genet* 2023; 68: 131–152.
5. Philips T and Rothstein JD. Rodent models of amyotrophic lateral sclerosis. *Curr Protoc Pharmacol* 2015; 69: 5.67.1–21.
6. Wijesekera LC and Leigh PN. Amyotrophic lateral sclerosis. *Orphanet J Rare Dis* 2009; 4: 3.
7. Dupuis L, Gonzalez de Aguilar JL, Oudart H, et al. Mitochondria in amyotrophic lateral sclerosis: a trigger and a target. *Neurodegener Dis* 2004; 1: 245–254.
8. Weydt P, Hong SY, Kliot M, et al. Assessing disease onset and progression in the SOD1 mouse model of ALS. *Neuroreport* 2003; 14: 1051–1054.
9. Docampo-Seara A, Santos-Durán GN, Candal E, et al. Expression of radial glial markers (GFAP, BLBP and GS) during telencephalic development in the catshark (*Scyliorhinus canicula*). *Brain Struct Funct* 2019; 224: 33–56.
10. Kipp M, Clarner T, Gingele S, et al. Brain lipid binding protein (FABP7) as modulator of astrocyte function. *Physiol Res* 2011; 60: S49–S60.
11. Kipp M, Gingele S, Pott F, et al. BLBP-expression in astrocytes during experimental demyelination and in human multiple sclerosis lesions. *Brain Behav Immun* 2011; 25: 1554–1568.
12. Sharifi K, Morihiro Y, Maekawa M, et al. FABP7 Expression in normal and stab-injured brain cortex and its role in astrocyte proliferation. *Histochem Cell Biol* 2011; 136: 501–513.
13. Louis DN, Ohgaki H, Wiestler OD, et al. The 2007 WHO classification of tumours of the central nervous system. *Acta Neuropathol* 2007; 114: 97–109.
14. Balendiran GK, Schnutgen F, Scapin G, et al. Crystal structure and thermodynamic analysis of human brain fatty acid-binding protein. *J Biol Chem* 2000; 275: 27045–27054.
15. Han X, Li H, Zhang Y, et al. Brain lipid-binding protein promotes proliferation and modulates cell cycle in C6 rat glioma cells. *Int J Oncol* 2017; 51: 1439–1448.
16. Tiwari A and Hayward LJ. Mutant SOD1 instability: implications for toxicity in amyotrophic lateral sclerosis. *Neurodegener Dis* 2005; 2: 115–127.
17. Mackenzie IRA, Bigio EH, Ince PG, et al. Pathological TDP-43 distinguishes sporadic amyotrophic lateral sclerosis from amyotrophic lateral sclerosis with SOD1 mutations. *Ann Neurol* 2007; 61: 427–434.
18. Deng HX, Zhai H, Bigio EH, et al. FUS-immunoreactive inclusions are a common feature in sporadic and non-SOD1 familial amyotrophic lateral sclerosis. *Ann Neurol* 2010; 67: 739–748.

19. Maruyama H, Morino H and Kawakami H. Causative genes for amyotrophic lateral sclerosis. *Brain Nerve* 2016; 68: 1081–1086.
20. Zhang J, Huang P, Wu C, et al. Preliminary observation about alteration of proteins and their potential functions in spinal cord of SOD1 G93A transgenic mice. *Int J Biol Sci* 2018; 14: 1306–1320.
21. Owada Y. Fatty acid binding protein: localization and functional significance in the brain. *Tohoku J Exp Med* 2008; 214: 213–220.
22. Liu RZ, Mita R, Beaulieu M, et al. Fatty acid binding proteins in brain development and disease. *Int J Dev Biol* 2010; 54: 1229–1239.
23. Anthony TE, Mason HA, Gridley T, et al. Brain lipid-binding protein is a direct target of Notch signaling in radial glial cells. *Genes Dev* 2005; 19: 1028–1033.
24. Arai Y, Funatsu N, Numayama-Tsuruta K, et al. Role of Fabp7, a downstream gene of Pax6, in the maintenance of neuroepithelial cells during early embryonic development of the rat cortex. *J Neurosci* 2005; 25: 9752–9761.
25. Ebrahimi M, Yamamoto Y, Sharifi K, et al. Astrocyte-expressed FABP7 regulates dendritic morphology and excitatory synaptic function of cortical neurons. *Glia* 2016; 64: 48–62.
26. Kagawa Y, Yasumoto Y, Sharifi K, et al. Fatty acid-binding protein 7 regulates function of caveolae in astrocytes through expression of caveolin-1. *Glia* 2015; 63: 780–794.
27. Li H, Jin G, Qin J, et al. Identification of neonatal rat hippocampal radial glia cells in vitro. *Neurosci Lett* 2011; 490: 209–214.
28. Bannerman P, Hahn A, Soulika A, et al. Astrogliosis in EAE spinal cord: derivation from radial glia, and relationships to oligodendroglia. *Glia* 2007; 55: 57–64.
29. Chaves-Filho AB, Pinto IFD, Dantas LS, et al. Alterations in lipid metabolism of spinal cord linked to amyotrophic lateral sclerosis. *Sci Rep* 2019; 9: 11642.
30. Rojas CV, Martínez JI, Flores I, et al. Gene expression analysis in human fetal retinal explants treated with docosahexaenoic acid. *Invest Ophthalmol Vis Sci* 2003; 44: 3170–3177.
31. Stillwell W and Wassall SR. Docosahexaenoic acid: membrane properties of a unique fatty acid. *Chem Phys Lipids* 2003; 126: 1–27.
32. Mita R, Coles JE, Glubrecht DD, et al. B-FABP-expressing radial glial cells: the malignant glioma cell of origin? *Neoplasia* 2007; 9: 734–744.
33. Mita R, Beaulieu MJ, Field C, et al. Brain fatty acid-binding protein and omega-3/omega-6 fatty acids: mechanistic insight into malignant glioma cell migration. *J Biol Chem* 2010; 285: 37005–37015.
34. De Rosa A, Pellegatta S, Rossi M, et al. A radial glia gene marker, fatty acid binding protein 7 (FABP7), is involved in proliferation and invasion of glioblastoma cells. *PLoS One* 2012; 7: e52113.
35. Liu RZ, Monckton EA and Godbout R. Regulation of the FABP7 gene by PAX6 in malignant glioma cells. *Biochem Biophys Res Commun* 2012; 422: 482–487.
36. Brun M, Coles JE, Monckton EA, et al. Nuclear factor I regulates brain fatty acid-binding protein and glial fibrillary acidic protein gene expression in malignant glioma cell lines. *J Mol Biol* 2009; 391: 282–300.

## Author biography

Qi Zhou holds a PhD and MD in Neurology. His area of research is amyotrophic lateral sclerosis.

Qing Kang holds an MS in Neurology. Her area of research is amyotrophic lateral sclerosis.

Wenzhi Chen holds a PhD and MD in Neurology. His area of research is amyotrophic lateral sclerosis and Parkinson's disease.

Renshi Xu is a professor in Neurology. His area of research is neurology focusing on amyotrophic lateral sclerosis and Parkinson's disease.